



Inter-comparison of model, satellite and in situ tropical cyclone heat potential in the North Indian Ocean

Babita Jangir¹ · D. Swain¹ · Samar Kumar Ghose¹ · Rishav Goyal¹ · T. V. S. Udaya Bhaskar²

Received: 19 April 2018 / Accepted: 14 August 2019 / Published online: 22 August 2019
© Springer Nature B.V. 2019

Abstract

The North Indian Ocean (NIO) experiences frequent tropical cyclones (TCs). TC heat potential (TCHP) is a major ocean parameter responsible for TC genesis and intensification changes. In this study, Indian National Centre for Ocean Information Services-Global Ocean Data Assimilation System (INCOIS-GODAS) model and satellite-derived TCHP data from National Remote Sensing Centre (NRSC) and National Oceanic and Atmospheric Administration (NOAA) are validated against TCHP from in situ profiles in the NIO during the period 2011–2013 for buoys and during 2005–2015 for Argo data. Data from eight moored buoys (6 in Bay of Bengal and 2 in Arabian Sea) under the Ocean Moored Buoy Network are used. Comparison of model and in situ TCHP yields correlation coefficients (root-mean-square errors in kJ/cm^2) of 0.74 (17.75), 0.59 (15.34), 0.70 (17.68), 0.60 (22.24), 0.57 (19.52), 0.73 (17.88) and 0.77 (39.17) at buoy locations BD08, BD09, BD10, BD11, BD13, AD06 and AD10. The scatter indices between collocated TCHP values at these locations were 0.32, 0.22, 0.30, 0.30, 0.31, 0.58 and 0.41. Further, it was found that satellite-based TCHP from NRSC match better with in situ as compared to near-real-time TCHP data obtained from NOAA. TCHP from INCOIS-GODAS model, NOAA delayed time data and NRSC TCHP data set are also in good agreement with those from Argo profiles. As a case study, model and in situ TCHP were compared during a TC, “Thane” at two buoy locations (BD11 and BD13), closest to its track. The analysis revealed underestimation of model TCHP at BD11, but good correlation at BD13. This could be attributed to the existence of a strong temperature inversion at BD11. It is observed that although the model is able to capture features like barrier and inversion layers, the temperature and depth of such layers are underestimated. Further, the recovery time from the influence of TC on the ocean subsurface is also much longer in case of the model which thus needs to be fine-tuned. Seasonal comparison of TCHP from various sources with in situ estimated TCHP also shows better correlation between all the products for the pre-summer monsoon compared to the post-summer monsoon season.

Keywords Tropical cyclone heat potential · OMNI buoy · Tropical cyclone · Cyclone Thane

✉ Babita Jangir
bj11@iitbbs.ac.in

Extended author information available on the last page of the article

1 Introduction

Tropical cyclone (TC) is considered as most devastating natural hazard in weather system. TCs pose severe threat to human life and property with implications on socio-economic aspects. It is very difficult to evacuate people at the time of such extreme events. So, real-time prediction of TC track and intensity is very necessary and has been a challenging problem for decades (Jangir et al. 2016). Ocean provides necessary energy in the form of ocean heat content (OHC) for TC genesis and intensification (Emanuel 1988). Many factors such as sea surface temperature (SST), eddies and OHC are important parameters for TC genesis. TC heat potential (TCHP), an estimate of OHC available for cyclone–ocean interaction, is defined as the sum of heat energy from ocean surface to 26 °C isotherm (Leipper and Volgenau 1972; Gray 1979; Swain and Krishnan 2013). Although the relation between SST and cyclone intensity (CI) is well established, a better forecast of CI requires considering the interactions of subsurface parameters such as OHC or TCHP. The National Hurricane Centre Statistical Hurricane Intensity Prediction Scheme (DeMaria and Kaplan 1994; DeMaria et al. 2005) and the Statistical Typhoon Intensity Prediction Scheme (Knaff et al. 2005) have shown that considering TCHP than SST alone yields a better forecast of TC intensity and track through models (Goni 2008; Goni et al. 2009). Improving the intensity and track forecast of TCs by models requires improvement of existing input forcing and their parameterizations. Most of the existing cyclone forecast models consider SST as their primary inputs (Ali et al. 2013). However, Ali et al. (2013) proposed inclusion of ocean subsurface parameters such as TCHP as well into the cyclone forecast models. Regular inclusion of the best available TCHP data in TC prediction models needs validation of various available data sets against in situ observations for better accuracy and reliability.

Conventionally, though TCHP can be best computed from in situ profiles of temperature and salinity (to account for density variations with depth), they have spatial and temporal limitations. In such cases, model-simulated or satellite-derived data could serve as useful alternatives. However, satellite-derived or model TCHP values need regional validation with available in situ estimates for quantification of their reliability and consistency (Nagamani et al. 2012). Following this, the satellite-derived TCHP with their better temporal and spatial resolutions can be used. The present work aims to inter-compare four sets of TCHP data sets, namely modelled TCHP from Indian National Centre for Ocean Information Services–Global Ocean Data Assimilation System (INCOIS-GODAS), satellite-based TCHP data sets procured from National Remote Sensing Centre (NRSC) and National Oceanic and Atmospheric Administration (NOAA) with TCHP computed from in situ profiles at certain buoy locations and Argo observations in the North Indian Ocean (NIO). Finally, a specific case for the Thane cyclone is studied utilizing model-derived and TCHP from buoys to analyse the reasons for any mismatch during a cyclone event.

2 Data and methodology

2.1 Study region

NIO (0–30°N and 40–100°E) is home for severe depressions and nearly 7% of worldwide TCs form in this region. Besides, an incredible number of cyclones form in the Bay of Bengal (BoB) than in the Arabian Sea (AS) (around four times higher) (Dube et al. 1997).

But the actual physics behind the cause of this is still unknown. Every year, nearly 5–6 TCs form in NIO region, in which 2–3 are very severe cyclones (Singh et al. 2001) and others are in the form of depressions or deep depressions. Hence, NIO is chosen as our study area. TCs form mostly during two seasons, such as pre-monsoon (March–May) and post-monsoon (October–December). Every year, the NIO cyclone season extends roughly between April and December with two peaks in May and November. This season includes cyclones in BoB and AS (Singh et al. 2001). Several studies have revealed that the frequency of severe TCs is increasing in the NIO region (Singh et al. 2000, 2001; Singh 2007; Srivastav et al. 2000; Sumesh and Ramesh 2013). Studies have also shown the importance of TCHP in TC genesis and intensification for different ocean basin (Wada and Usai 2007; Mainelli et al. 2008; Wada et al. 2012), but very few studies have been carried out for the NIO region (Sadhuram et al. 2006; Ali et al. 2007, 2010, 2012a, b; Sharma et al. 2013; Vissa et al. 2013; Sharma and Ali 2014; Kumar and Chakraborty 2011). Though the works by George and Gray (1976), Goni et al. (1996), Gilson et al. (1998), Mayer et al. (2001) and Willis et al. (2004) discussed the role of TCHP on cyclone intensification, none of them clearly indicate that which data set is better for cyclone-related studies in the NIO region. This is essential to minimize the error associated with cyclone forecast in this region. Nagamani et al. (2012) attempted validation of only satellite-derived TCHP by inter-comparison with in situ TCHP data. In our study, we have attempted to validate multiple TCHP data sets including model with TCHP from in situ measurements for the NIO region, ranging from 3-year to 10-year period.

2.2 Data used

2.2.1 Moored buoy observations

The in situ temperature and salinity data from moored buoys during the years 2011–2013 have been obtained from INCOIS, and their spatial distribution in the study area is shown in Fig. 1. The in situ data sources consisted of moored buoys deployed under the OMNI (Ocean Moored Buoy Network for NIO) programme spanning the time period 2011–2013

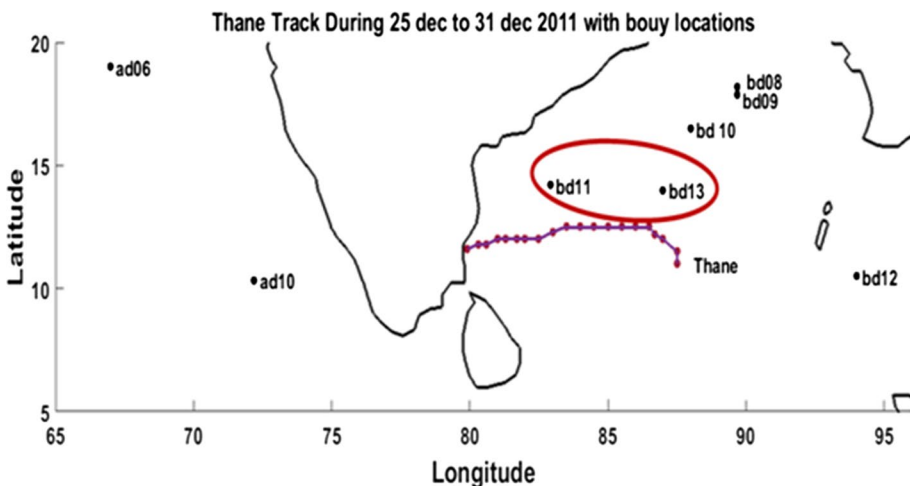


Fig. 1 Buoy locations in the study area and track of cyclone Thane

(Source; INCOIS, Hyderabad). This analysis period has been selected considering the maximum availability of continuous data at all the buoy locations.

The OMNI buoys are attached with sensors to continuously measure surface and sub-surface met-ocean parameters like air temperature, rainfall, wind speed, air pressure, wind gust, temperature and salinity profiles, currents, etc., on real-time basis. Vertical profiles of temperature and salinity are recorded till 500 m depth. The OMNI buoy programme has served as a very useful data resource for understanding the observed variability of upper ocean thermohaline and current structures on several timescales over the years (Venkatesan et al. 2013). The OMNI buoy temperature and salinity profiles are available at hourly temporal intervals and have been used to compute TCHP (henceforth represented as TCHP_I).

2.2.2 Model-simulated TCHP (TCHP_M)

TCHP data are also obtained from INCOIS-GODAS model for the period 2005–2015. These are at $1^\circ \times 1^\circ$ and 6-hour spatial and temporal resolutions, respectively. The INCOIS-GODAS, a modified version of National Centre for Environmental Prediction-GODAS (NCEP-GODAS), is an Ocean General Circulation Model based on Modular Ocean Model-4.0 (www.incois.gov.in/portal/GODAS) with 3DVAR assimilation scheme and Newtonian relaxation (Ravichandran et al. 2013). The global ocean analysis of temperature, salinity, sea surface height anomaly (SSHA) and currents from surface to the bottom of the ocean has been provided every day by INCOIS-GODAS on real-time basis (products with 1-day delay). Various products such as El-Nino indices, global maps of monthly SST anomalies, depth-wise distribution of temperature anomalies and TCHP are also being made available using the INCOIS-GODAS ocean analysis (www.incois.gov.in/portal/GODAS). In our analysis, the INCOIS-GODAS model-simulated TCHP is denoted by TCHP_M.

2.2.3 Satellite-based TCHP

TCHP data obtained from two other sources, namely NRSC (TCHP_A) and NOAA (TCHP_{NRT} denoting near-real-time TCHP and TCHP_{DT} denoting delayed time TCHP products), utilized in our analysis are based on computation of TCHP from satellite-observed parameters. The details of these data sets are provided in the succeeding subsections.

(a) NRSC TCHP (TCHP_A)

TCHP_A is daily products with $0.25^\circ \times 0.25^\circ$ spatial resolution. TCHP_A is estimated using SSHA from available altimeters, SST from Tropical Rainfall Measuring Mission-Microwave Imager (TRMM-TMI) and the climatological values of the 26 °C isotherm using artificial neural network approach (Ali et al. 2012a, b; Kashyap et al. 2012). It is generated on a daily basis from 1998 to present with a 1-week time delay. We have considered TCHP_A for the period 2005–2015 for our analysis.

(b) NOAA TCHP (TCHP_{NRT} and TCHP_{DT})

TCHP (version 2.1) obtained from NOAA is also a satellite product freely made available by the Atlantic Oceanographic and Meteorological Laboratory (www.aoml.noaa.gov/phod/cyclone; Pun et al. 2007; Harwood and Scarrott 2013). The data are available in two modes, near-real-time products (TCHP_{NRT}: updated monthly with 1-month delay from

the satellite pass) and delayed time products (TCHP_{DT}: updated monthly with a 6-month delay), both available at 0.25°×0.25° spatial resolution. TCHP_{NRT} fields are produced using near-real-time AVISO sea surface height anomaly (SSHA) gridded fields that merge all available satellite observations using an optimal interpolation technique and hence may be more relevant for cyclone-related studies, whereas TCHP_{DT} products are of weekly temporal resolution and are produced using delayed time AVISO SSHA gridded fields that merge all available satellite observations using an optimal interpolation technique.

2.2.4 Cyclone best track data

CI is a representation of the maximum sustained wind (MSW) of a cyclone (Chen 2009). For TC Intensity, best track data made available by Indian Meteorological Department (IMD) at 3-hour time intervals are used (<http://www.rsmcnewdelhi.imd.gov.in/images/pdf/archive/best-track/besttrack.pdf>). Table 1 presents details of data used for this analysis.

2.2.5 Argo observation (TCHP_{argo})

Daily Argo temperature and salinity profiles are collected and made freely available by the International Argo Program (IAP) and the national programmes that contribute to it (<http://www.argo.ucsd.edu>) for the period 2005–2015 and used after quality control (Wong et al. 2009).

2.3 Methodology

Conventionally, TCHP is computed from in situ subsurface temperature and salinity profiles using the expression given by Leipper and Volgenau (1972) as:

$$\text{TCHP} = \int_0^{D26} \rho C_p (T - 26) dz \quad (1)$$

where density (ρ) is the layer density of the seawater, C_p is the specific heat capacity of seawater at constant pressure p , T is the temperature (°C) of each layer of dz thickness and $D26$ is the depth of the 26 °C isotherm in the ocean. When the SST is below 26 °C, TCHP for the layer is assumed to be zero (Nagamani et al. 2012). ρ is a function of temperature and salinity, and C_p is a function of salinity, temperature and pressure (Fofonoff and Millard 1983). In Eq. (1), density (ρ) and specific heat capacity (C_p) have been computed using United Nations Educational, Scientific, Cultural Organization (UNESCO) equation of state

Table 1 Details of various data sets used in the present work

Data	Source	Resolution	Satellite/model/in situ	Period
TCHP	INCOIS	1°×1° (6 hourly)	INCOIS-GODAS model	2005–2015
	NRSC	0.25°×0.25° (Daily)	Satellite	
	NOAA	0.25°×0.25° (Daily)	Satellite	
Cyclone best track	IMD	(3 hourly)	Observational data	25/12/2011–30/12/2011
Buoy T/S profiles	INCOIS	Hourly	In situ	2011–2013
Argo	IAP	Daily	In situ	2005–2015

of seawater (Millero et al. 1980; Millero and Poisson 1981; Fofonff and Millard 1983). A comparative analysis has been made between the model and satellite obtained data sets with reference to TCHP obtained from buoy measurements. The work concludes with a case study for cyclone “Thane” (25 December to 31 December 2011) at nearby buoy locations, BD11 and BD13 in the BoB. As a first part of our analysis, we have validated TCHP from various sources (model and satellite) by inter-comparison with in situ values. Following this, the suitability of INCOIS-GODAS TCHP data set is evaluated during a very severe cyclonic storm “Thane” as a case study.

3 Results and discussion

With the primary objective of arriving at the best alternative TCHP data that can be utilized for cyclone-related studies in the absence or to overcome the basic limitations of in situ observations, TCHP from various sources is analysed and inter-compared with TCHP estimated from in situ profiles in the NIO. The results from this analysis and inferences drawn are presented in the subsequent sections.

3.1 Inter-comparison of $TCHP_M$ and $TCHP_I$

For the inter-comparison of $TCHP_M$ and $TCHP_I$, $TCHP_I$ has been calculated using Eq. 1 from temperature and salinity profiles at 8 OMNI buoys locations followed by statistical analysis during the period 2011–2013. As $TCHP_I$ are hourly products and $TCHP_M$ data are available at every 6 h, they have been taken for the matching times and spatially collocated for validation using nearest neighbour technique suggested by Dacey (1960). Analysis has been carried out at each buoy location, namely BD08 (89°E, 18°N), BD09 (89.69°E, 17.89°N), BD10 (88°E, 16°N), BD11 (83°E, 14°N), BD12 (94°E, 10°N) and BD13 (86°E, 11°N) in the BoB and AD06 (67.50°E, 10.30°N) and AD10 (72.20°E, 10.33°N) in the AS (Fig. 1).

The buoy locations are chosen to cover the maximum spatial heterogeneity in the sub-surface heat content as well as the study area to the best possible extent. The dynamics in NIO, especially in BoB, varies rapidly from the south to the head Bay. The head Bay is mostly affected by the land and the huge water influx from five major rivers, particularly during the monsoons. The buoys BD08, BD09 and BD10 represent the head Bay. The central and the southern Bay are mostly affected by the monsoonal dynamics as well as the large influx of heat from the Malacca strait via the Indonesian Through-Flow (ITF) channel (Sengupta et al. 2006; Valsala and Ikeda 2005; Song et al. 2003). In addition, Inter-decadal Pacific Oscillations (IPO) phases and El-Nino/La-Nina conditions also affect the BoB dynamics. The central part of the Bay is represented by BD11 and BD13, and buoy BD12 represents the south-eastern part of the Bay. In the AS, two available OMNI buoys (AD10 and AD06) are considered which represent the AS Mini Warm Pool (ASMWP) and northernmost AS (Fig. 1).

The scatters between $TCHP_M$ and $TCHP_I$ are shown for BoB in Fig. 2, and Fig. 3 presents the scatters for the AS. The detailed statistical parameters are presented in Table 2. A high positive correlation ($r \geq 0.7$) between the model estimates and in situ TCHP is observed at BD08 (RMSE: 17.75 kJ/cm²), BD10 (RMSE: 17.68 kJ/cm²), AD06 (RMSE: 17.88 kJ/cm²) and AD10 (RMSE: 39.17 kJ/cm²) locations. The value of r (and mean absolute error (MAE)) is 0.74 (and 14.05 kJ/cm²), 0.70 (and 14.28 kJ/cm²), 0.73 (and 10.83 kJ/cm²)

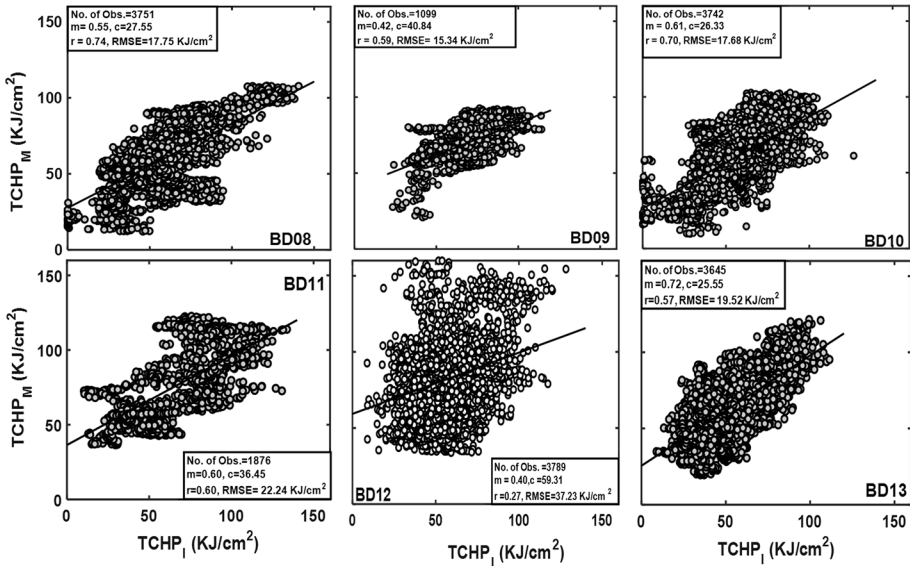


Fig. 2 Scatters of buoy estimated and INCOIS-GODAS model TCHP during 2011–2013 in the Bay of Bengal

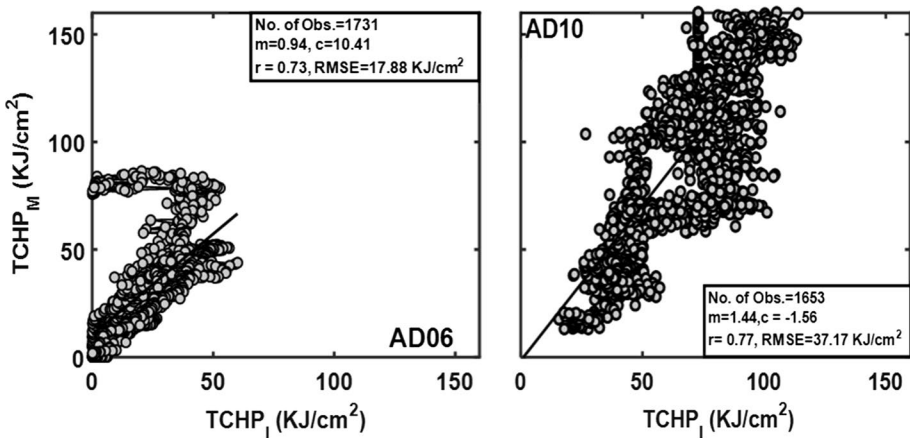


Fig. 3 Scatters of buoy estimated and INCOIS-GODAS model TCHP during 2011–2013 in the Arabian Sea

cm²) and 0.77 (and 31.69 kJ/cm²), respectively, for each of the above buoys. At other buoy locations, *r* is relatively lower at 0.59, 0.60 and 0.57 for the buoys BD09, BD11 and BD13, respectively, with the least correlation (*r*=0.27) at BD12. Similarly, RMSE and MAE (in kJ/cm²) at these buoy locations are 15.34 and 13.01 (BD09), 22.24 and 17.46 (BD11), 37.23 and 28.28 (BD12), and 19.52 and 15.66 (BD13). The scatter index (SI, which is the RMSE normalized by the mean measured value (Zambresky 1989) at each buoy location for the above comparison was obtained to be 0.32 (BD08), 0.22 (BD09), 0.30 (BD10 and BD11), 0.45 (BD12), 0.31 (BD13), 0.58 (AD06) and 0.41 (AD10) as shown in Table 2.

Table 2 Statistics of inter-comparison between TCHP estimated from buoys and that of INCOIS-GODAS model at the buoy locations in the North Indian Ocean

Buoy	Lat. (°N)	Lon. (°E)	No. of obs.	In situ		Model		<i>r</i>	RMSE	Bias	MAE	SI
				Range	SD	Range	SD					
BD08	18.18	89.68	3751	1–141	22.17	9–108	22.64	0.74	17.75	–2.93	14.05	0.32
BD09	17.86	89.68	1099	23–114	13.20	21–93	18.87	0.59	15.34	–2.21	13.01	0.22
BD10	16.50	88.00	3742	0–127	22.30	10–103	20.74	0.70	17.68	–1.60	14.28	0.30
BD11	14.21	82.91	1876	10–114	22.54	36–123	27.50	0.60	22.24	–7.08	17.46	0.30
BD12	10.50	94.00	3789	9–128	26.34	34–179	17.95	0.27	37.23	–25.08	28.28	0.45
BD13	13.99	87.00	3645	9–111	20.29	20–121	19.23	0.57	19.52	–12.14	15.66	0.31
AD06	19.00	66.98	1731	1–60	22.16	0–86	14.74	0.73	17.88	–5.42	10.83	0.59
AD10	10.33	72.19	1653	16–114	40.31	13–165	21.41	0.77	39.17	–27.78	31.69	0.41

SD standard deviation; *RMSE* root-mean-square error; *MAE* mean absolute error; *SI* scatter index

On considering the above statistical parameters, the in situ TCHP derived from buoys BD08, BD09, BD10, BD11 and BD13 ($SI \approx 0.30$ and $r^2 \approx 0.5$) model data has best match with in situ in BoB except for BD12 ($SI = 0.45$ and $r = 0.27$). Further, good correlation ($r \geq 0.7$) is observed even at the buoy locations BD08 and BD10 which are present in the head Bay. The correlation ($r \leq 0.3$) which is the least at BD12 (south-eastern BoB) along with other statistical comparison metrics could possibly imply that the model is unable to capture short-duration variabilities resulting from the ITF in this region.

Similarly, in the AS, a good correlation ($r \geq 0.7$) is observed between model and in situ TCHP data at both the buoy locations (AD06 and AD10), but SI is relatively high ($SI \geq 0.40$). Qualitatively, it can be mentioned that model TCHP shows a better match with in situ at AD10 location (ASMWP) in comparison with AD06 (northern AS). TCHP data obtained from INCOIS-GODAS model exhibit better match with in situ in the AS region considered which could be owing to the better capabilities of an Ocean General Circulation Model in simulating the vertical structure of the ocean.

The INCOIS-GODAS uses a global Ocean General Circulation Model, Modular Ocean Model-4.0, with 3DVAR assimilation technique (Griffies et al. 1998; Ravichandran et al. 2013). The model assimilates all the available in situ observations (Argo, Buoys and ship based) of temperature and salinity profile up to 700 m. It uses a Newtonian relaxation scheme, and the model SST is nudged towards the satellite-based gridded observations. As in model data, in situ observation has been used to compute temperature and salinity profile, the model TCHP has better correlation at most of the buoy locations except one at south-eastern BoB (BD12). This leads to the possible conclusion that the model may not capture ITF well enough in the south-eastern BoB.

3.1.1 Inter-comparison of satellite and in situ TCHP products (TCHP_A, TCHP_{NRT}, TCHP_{DT} and TCHP_I)

It was observed from the earlier subsection that TCHP_M has good positive correlation with TCHP_I for most of the buoy locations excluding BD12. In order to examine the suitability of TCHP obtained from satellites, TCHP from NRSC (TCHP_A) and NOAA (TCHP_{NRT} (near real time) and TCHP_{DT} (delayed time) were compared with TCHP_I. The statistical details of comparison of correlation coefficient and RMSE are shown in Table 3. The r values for TCHP_A and TCHP_I are found to be 0.75 (BD08), 0.83 (BD09), 0.84 (BD10), 0.54 (BD11), 0.51 (BD12), 0.57 (BD13), 0.64 (AD06) and 0.75 (AD10), and RMSE values (in kJ/cm^2) at these buoy locations are 18.89 (BD08), 11.84 (BD09), 14.36 (BD10), 33.90 (BD11), 20.55 (BD12), 22.55 (BD13), 18.55 (AD06) and 21.95 (AD10). Thus, it is observed that $r \geq 0.5$ at most of all buoys locations. The analysis shows that a good correlation exists between satellite and in situ TCHP in the head Bay and in AS. The correlations are rather poor in the southern Bay compared to head Bay.

For the comparison between TCHP_{NRT} (obtained from NOAA) and TCHP_I, r values are 0.53 (at BD08), 0.36 (BD09), 0.56 (BD10), 0.57 (BD11), 0.26 (BD12), 0.41 (BD13), 0.59 (AD06), and 0.72 (AD10). The RMSE values (in kJ/cm^2) are 28.46 (BD08), 29.26 (BD09), 25.86 (BD10), 30.80 (BD11), 23.67 (BD12), 25.13 (BD13), 21.61 (AD06) and 18.70 (AD10) (Table 3), whereas, for TCHP_{DT} and TCHP_I, r values are 0.64 (at BD08), 0.63 (BD09), 0.73 (BD10), 0.61 (BD11), 0.52 (BD12), 0.64 (BD13), 0.64 (AD06), and 0.74 (AD10). The RMSE values (in kJ/cm^2) are 24.87 (BD08), 19.96 (BD09), 19.44 (BD10), 30.13 (BD11), 19.30 (BD12), 20.88 (BD13), 15.87 (AD06) and 21.24 (AD10). It is clearly seen that r is positive at most of the buoy locations ($r \geq 0.5$ for TCHP_{DT}), but this is not

Table 3 Statistical metrics of inter-comparisons of TCHP from various sources with buoy-derived TCHP in the North Indian Ocean

	BD08	BD09	BD10	BD11	BD12	BD13	AD06	AD10
Corr. Coeff.								
TCHP _M	0.74	0.59	0.70	0.60	0.27	0.57	0.73	0.77
TCHP _A	0.75	0.83	0.84	0.54	0.51	0.57	0.64	0.75
TCHP _{NRT}	0.53	0.36	0.56	0.57	0.26	0.41	0.59	0.72
TCHP _{DT}	0.64	0.63	0.73	0.61	0.52	0.64	0.64	0.74
RMSE (kJ/cm ²)								
TCHP _M	17.75	15.34	17.68	22.24	37.23	19.52	17.88	39.17
TCHP _A	18.89	11.84	14.36	33.90	20.24	22.55	18.69	21.95
TCHP _{NRT}	28.46	29.26	25.86	30.80	23.67	25.13	21.61	18.70
TCHP _{DT}	24.87	19.96	19.44	30.13	19.30	20.88	15.87	21.24

true for TCHP_{NRT}. At buoy BD09, BD12 and BD13, the value of r is less than 0.5. It is also observed from the analysis that even though TCHP_{NRT} and TCHP_{DT} both are positively correlated with TCHP_I, r is less for TCHP_{NRT} data set compared to TCHP_{DT} (Table 3).

One possible reason for different r values for TCHP_M, TCHP_A, TCHP_{NRT} and TCHP_{DT} with TCHP_I could also be the difference in TCHP computation methodology. Satellite-based TCHP is computed globally from altimeter-derived vertical temperature profiles and satellite SST and hence is strongly correlated with SSHA (Harwood and Scarrott 2013). The difference among the various satellite and in situ TCHP products could also be due to the mismatch between the satellite and in situ observation times as well as spatial locations. Further, in all the data sets mentioned above (including TCHP_A), TCHP is estimated from satellite observations considering ρ and C_p as constant (Goni et al. 1997; Ali et al. 2012a, b; Kashyap et al. 2012; Harwood and Scarrott 2013), whereas we have considered them as variables computed following Fofonff and Millard (1983) accounting for the contribution of salinity to variations in density and C_p in the TCHP computation Eq. (1). It is well known that salinity influences the density differently in different ocean basins and the salinity variations are appreciable in the Bay of Bengal.

Finally, a combined comparison of model, satellite and in situ TCHP was carried out. Time series of differences of TCHP_M, TCHP_A, TCHP_{NRT}, TCHP_{DT} with respect to TCHP_I is shown in Figs. 4 (for BoB) and 5 (for AS). It is observed that even though the difference of TCHP time series follows a similar pattern at each of the buoy locations, the values in each case are quite different. It is further found that TCHP_{NRT} from NOAA is overestimated compared to all other TCHP data sets (Figs. 4, 5). However, Nagamani et al. (2012) in their analysis of TCHP_{DT} in the NIO and in situ Argo profiles found a good correlation ($r=0.65$) between the two data sets. They also observed that the correlation increased ($r=0.76$) on using monthly averaged TCHP data sets. On close analysis, it is observed that Nagamani et al. (2012) have used TCHP_{DT} products from NOAA in their analysis since 1993 to 2009. However, we have used NOAA TCHP_{NRT} data in our analysis. When we analysed using TCHP_{DT}, we also obtained positive correlations ($r \geq 0.5$) between TCHP_{DT} and TCHP_I for all the buoys in line with that of Nagamani et al. (2012). However, although positive, the correlation values are lower for TCHP_{NRT} compared to TCHP_{DT}. This difference may be interpreted

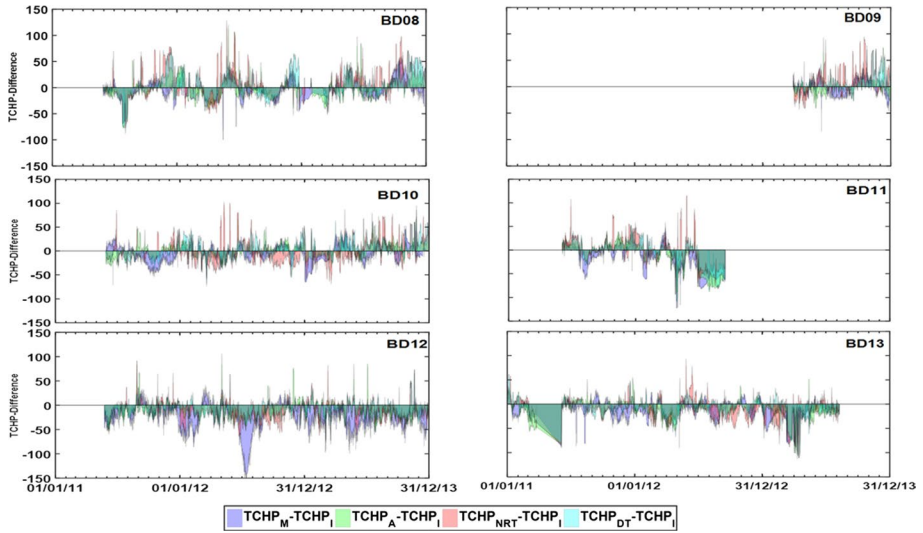


Fig. 4 Plots of differences between various TCHP products and buoy estimated TCHP in the Bay of Bengal

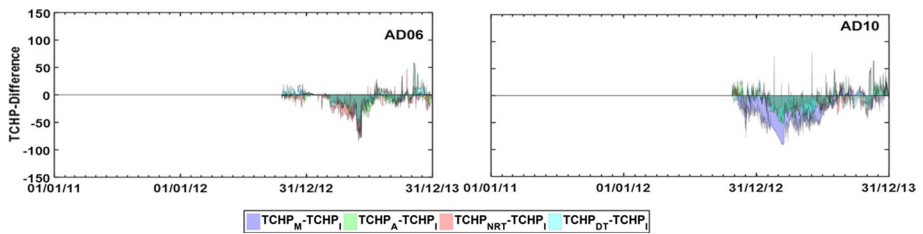


Fig. 5 Plots of differences between various TCHP products and buoy estimated TCHP in the Arabian Sea

as satellite’s inability to capture accurately the daily ocean subsurface variability, whereas monthly averaging reduces these errors.

It is to be further noted that since satellite products are only available as daily products on delayed mode, it is not feasible to obtain real-time TCHP for cyclone prediction purposes from satellites. On the other hand, model-simulated data are 6 hourly and can be generated on day-to-day basis as well as forecast mode. Conclusively, the state of weather can be well forecasted by using assimilated (real-time observations and model prediction) data as the input for cyclone prediction models. From our analysis of four TCHP products, it is also observed that INCOIS-GODAS model and NRSC TCHP data sets have better match with in situ TCHP, so these may be utilized for cyclone-related studies in NIO region in the absence of real-time in situ observations.

3.1.2 Inter-comparison of various TCHP products with TCHP from Argo (TCHP_{argo})

TCHP products obtained from various sources are also inter-compared with that computed from ARGO (TCHP_{argo}) in the NIO region for a decade long period (2005–2015) in the study region. It is observed from this analysis that correlation between TCHP_M, TCHP_A,

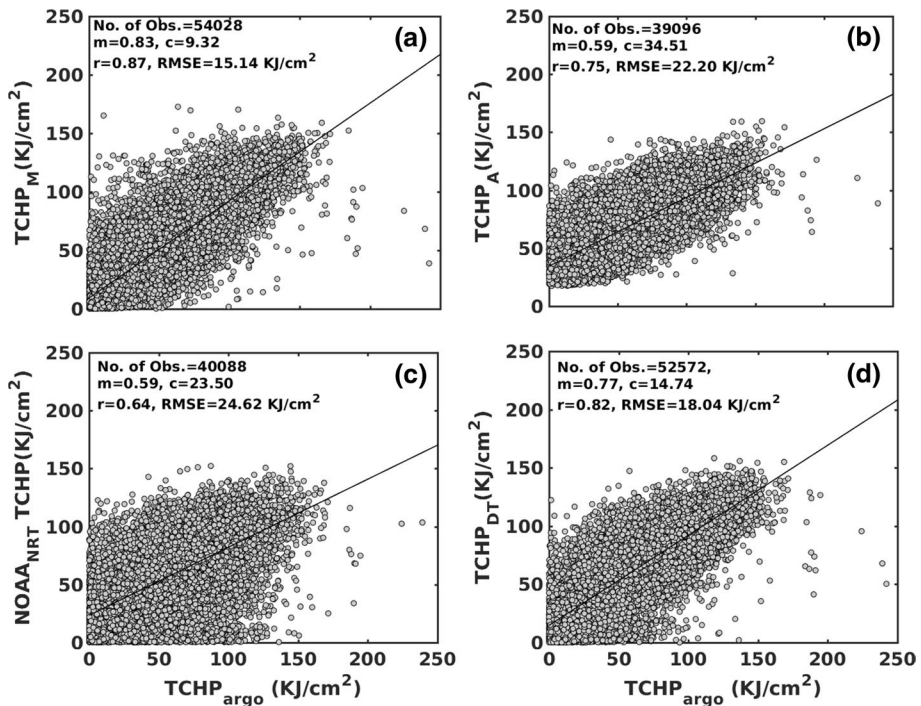


Fig. 6 Scatters between TCHP from ARGO and **a** INCOIS-GODAS model, **b** NRSC, **c** NOAA-NRT and **d** NOAA-DT during the period 2005–2015 in the North Indian Ocean

TCHP_{NRT} and TCHP_{DT} with TCHP_{argo} is 0.87, 0.75, 0.64 and 0.82, respectively, and the corresponding RMSE value is 15.14, 22.20, 24.62 and 18.04 (Fig. 6). As earlier, it is also observed from this comparison that TCHP_{NRT} is less correlated with TCHP_{argo} compared to all other data sets. TCHP was also compared with TCHP_{argo} for the two prominent cyclone seasons in the study region separating them into seasonal data sets to examine seasonal dependence of the correlations if any (Fig. 7). It is observed that the correlation between all the TCHP products with TCHP_{argo} is higher in the pre-summer monsoon season compared to the post-summer monsoon season.

3.2 Evaluation of TCHP data sets during a tropical cyclone: Thane

To evaluate the performance of TCHP_M as compared to TCHP_I during TCs, a case study has been carried out for Thane cyclone. The cyclonic storm “Thane” crossed the north-east district of Tamil Nadu coast on 30 December 2011. It was a very severe cyclone of category II, in which maximum sustained winds reached up to 140 km/h. The choice of this storm is also based on the data availability along the track of the storm, as two buoys, namely BD11 and BD13, were situated in its proximity. Therefore, the validation exercise was carried out at these two buoy locations. Table 4 represents statistical parameters such as r , RMSE and SI for inter-comparison between TCHP_M and TCHP_I for cyclone Thane. The correlation, bias, RMSE and SI between TCHP_M and TCHP_I at BD13 are

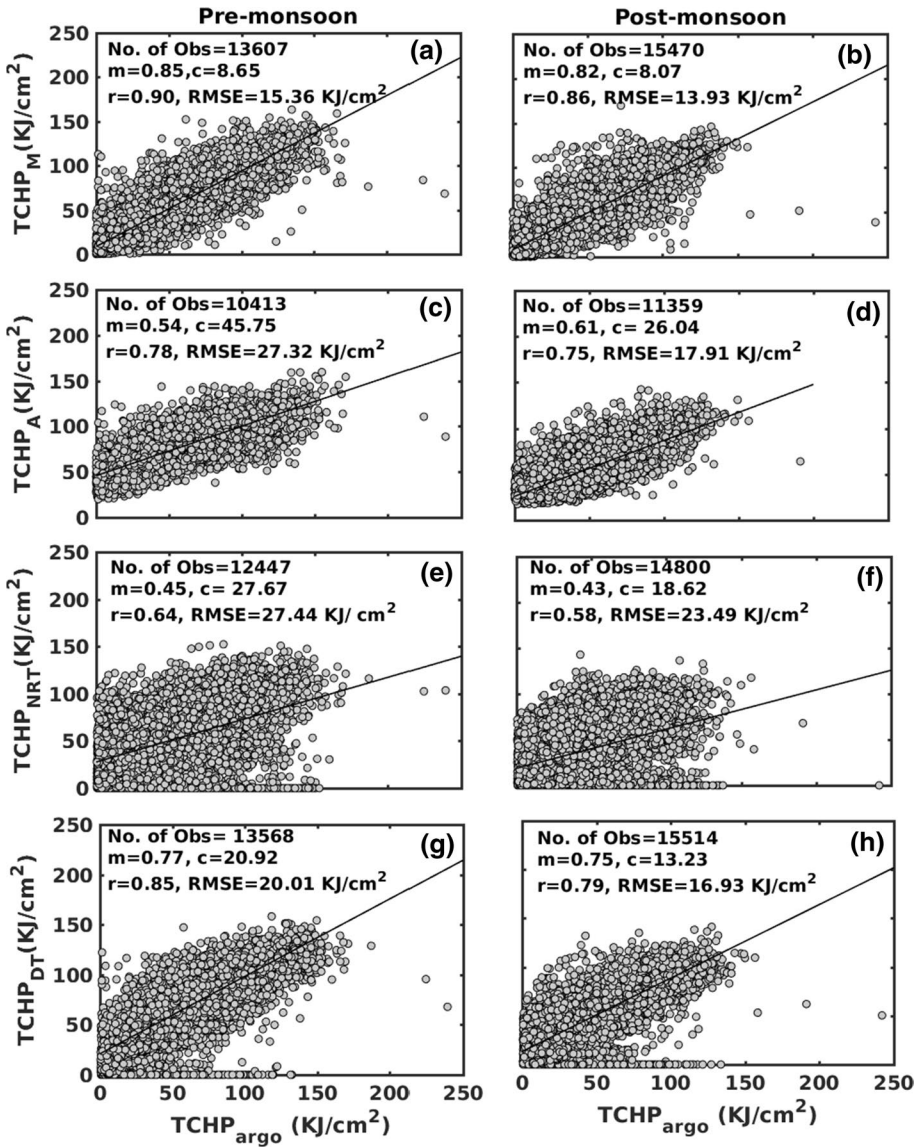


Fig. 7 Scatters between TCHP from ARGO and **a, b** INCOIS-GODAS model, **c, d** NRSC, **e, f** NOAA-NRT and **g, h** NOAA-DT for the two cyclone seasons (2005–2015) in the North Indian Ocean. The left panels are for the pre-summer monsoon, and right panels represent the post-summer monsoon

Table 4 Comparison statistics of TCHP from model and buoys during the passage of cyclone Thane (25 December 2011 to 30 December 2011)

Buoy	Lat. (°N)	Lon. (°E)	<i>r</i>	RMSE (in kJ/cm ²)	BIAS	SI
BD11	14.21	82.91	-0.15	12.30	-9.30	0.22
BD13	13.99	87.00	0.89	13.91	12.61	0.35

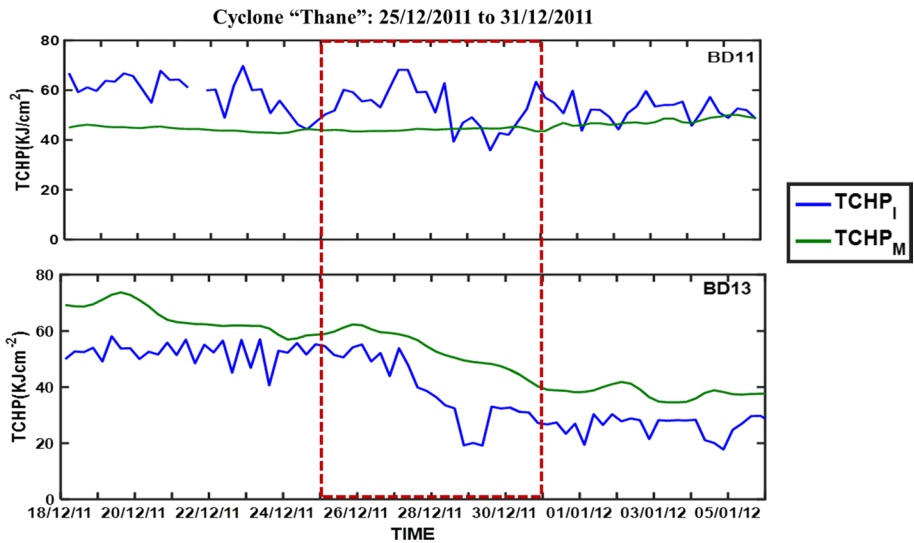


Fig. 8 Inter-comparison of INCOIS-GODAS and buoy estimated TCHP during the “Thane” cyclone at locations of BD11 and BD13 buoys (red dashed lines indicate TC Thane start and end dates)

0.89, 12.61 kJ/cm², 13.91 kJ/cm² and 0.35. At BD11, the correlation, bias, RMSE and SI between TCHP_M and TCHP_I are -0.15 , -9.30 kJ/cm², 12.30 kJ/cm² and 0.22 (Table 4). The negative bias in TCHP_M at BD11 shows underestimation of model data; at the same time, positive bias at BD13 shows overestimation of model data (Fig. 8). The red-coloured dashed lines in Fig. 8 represent the start and end days of cyclone considered at that buoy (duration when the cyclone passes nearer that buoy location). Both the TCHP products at BD11 show very small increase after the cyclone or nearly remain constant. However, at BD13, TCHP values show a decreasing trend after the pass of the cyclone.

Time series of temperature profiles at the two buoy locations ranging from 5 days before to 5 days after the cyclone period was analysed to investigate possible reason for observed mismatch between model and in situ TCHP data sets at the two buoy locations. A strong temperature inversion is observed at BD11 before the passage of Thane (Fig. 9). The layer then breaks during the cyclone passage, and the inversion layer reappears post this. It is possible that the presence of temperature inversions at the buoy BD11 location has resulted in negative r between TCHP_M and TCHP_I as the variation in the inversion in temperature profiles may not be well captured by the model (Fig. 9 and Table 4). As seen in the figure, the temperature as well as depth and thickness of the inversion layer is underestimated by the model compared to buoy data. Further, breaking of inversion layer during the passage of Thane cyclone is captured by the buoy data as well as model but the reformation of this layer after the passage of cyclone is not captured by the model at BD11, whereas at BD13, temperature is overestimated by the model (Fig. 9: right panels) and it is very well captured in buoy data. This can also be deduced from the positive r at buoy location BD13 where the inversions are absent in the temperature times series. This possibly points at the limitation of the model to represent the temperature inversions in the ocean subsurface accurately. These subsurface layers (such as inversion layer and barrier layer) play an important role in modifying

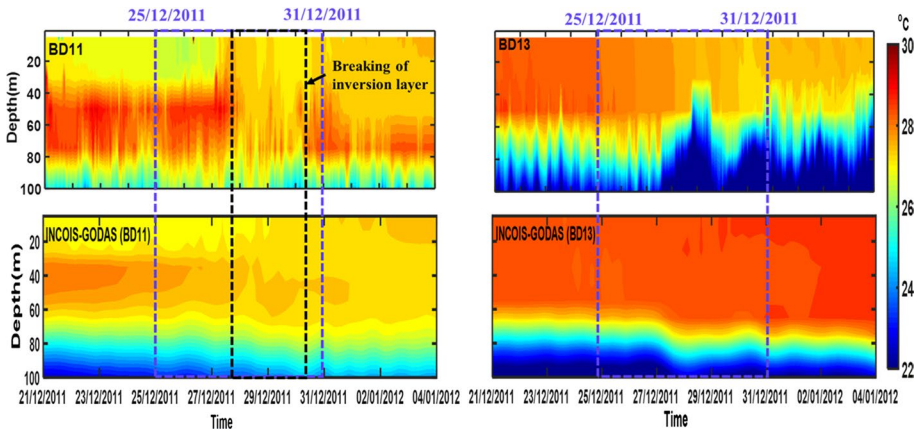


Fig. 9 Subsurface profiles of temperature from INCOIS-GODAS model and buoys at BD11 and BD13 buoy locations during passage of cyclone “Thane” (25 December 2011 to 30 December 2011). Blue dashed lines indicate TC Thane start and end dates

CI and their tracks. The subsurface is relatively warmer owing to the presence of inversion layers which could possibly be a reason for TC intensification due to availability of excess heat at such locations.

4 Conclusions

It is not possible to get buoy data (in situ) at every location; hence, this comparison helps to select alternate TCHP data products which could be as reliable as that obtained from in situ profiles. From this analysis, it is observed that $TCHP_M$ (model estimated) compares well with the in situ estimations at most of the buoy locations such as BD08, BD09, BD10, BD11 and BD13 in the BoB, and AD06 and AD10 in the AS. However, the correlation is observed to be rather poor at buoy BD12. It is also noticed that $TCHP_M$, $TCHP_A$ (TCHP estimated from NRSC) and $TCHP_{DT}$ follow similar pattern as in situ $TCHP_I$. The differences between $TCHP_{NRT}$ and $TCHP_I$ are large compared to differences between $TCHP_I$ and $TCHP_M$, $TCHP_A$ and $TCHP_{DT}$ at all buoy locations during the comparison period. This leads us to conclude that model-derived ($TCHP_M$) and satellite-derived NRSC products ($TCHP_A$) followed by $TCHP_{DT}$ are more reliable compared to $TCHP_{NRT}$ in the NIO region. However, model-derived data sets ($TCHP_M$) compare the best with in situ estimations among all the data sets analysed in the NIO region, except for south-eastern BoB, during the analysis period. In this region, $TCHP_M$ and $TCHP_I$ are also better correlated than other TCHP products.

A case study to evaluate the suitability of use of $TCHP_M$ during cyclones when in situ observation from buoys may not be available was carried out for TC Thane, and the statistical metrics of the comparison were analysed. Two buoy locations (BD11 and BD13) close to the cyclone track were selected for this. It was observed that $TCHP_M$ at BD11 is underestimated as compared to in situ data, but shows good correlation with $TCHP_I$ at BD13. The presence of inversion layer in the ocean subsurface at BD11 was determined to be main cause for this mismatch, accurate properties of which probably are not well captured by the model. So after rupturing the inversion layers during cyclonic activity, TC

intensifies due to the excess heat supplied by subsurface to surface as has also been concluded earlier by Balaguru et al. (2012). It can be one of the possible reasons for “Thane” cyclone to become a severe TC.

Acknowledgements The authors gratefully acknowledge Indian National Centre for Ocean Information Services (INCOIS) for the financial support and support from MoES and IIT Bhubaneswar for facilitating the execution of this research Project. TCHP data and buoy data were obtained from INCOIS, NOAA and NRSC and the cyclone best track data from IMD. The institutions are acknowledged for making the data available free of cost. One of the authors, BJ, was supported by a research fellowship by INCOIS under the Grant INCOIS:F&A:SSPDM:XII:A3:002 for carrying out this work.

References

- Ali MM, Jagadeesh PSV, Jain S (2007) Effects of eddies on Bay of Bengal cyclone intensity. *EOS Trans AGU* 88:93–95
- Ali MM, Goni GJ, Jayaraman V (2010) Satellite derived ocean heat content improves cyclone prediction. *Earth Obs Syst* 91:396–397
- Ali MM, Jagadeesh PSV, Lin II, Hsu J-Y (2012a) A neural network approach to estimate tropical cyclone heat potential in the Indian Ocean. *IEEE Geosci Remote Sens Lett* 9:1114–1117. <https://doi.org/10.1109/LGRS.2012.2190491>
- Ali MM, Jagadeesh PSV, Lin I-I, Hsu J-Y (2012b) A neural network approach to estimate tropical cyclone heat potential in the Indian Ocean. *IEEE Geosci Remote Sens Lett* 9:1114–1117. <https://doi.org/10.1109/LGRS.2012.2190491>
- Ali MM, Swain D, Kashyap T, McCreary JP, Nagamani PV (2013) Relationship between cyclone intensities and sea surface temperature in the tropical Indian Ocean. *IEEE Geosci Remote Sens Lett* 10:841–844
- Balaguru KP, Chang R, Saravanan LYR, Leung Z, Xu MLI, Hsieh J (2012) Ocean barrier layers: effect on tropical cyclone intensification. *Proc Natl Acad Sci USA* 109:14343–14347. <https://doi.org/10.1073/pnas.1201364109>
- Chen G (2009) Inter-decadal variation of tropical cyclone activity in association with summer monsoon, sea surface temperature over the western North pacific. *Chin Sci Bull* 54:1417–1421
- Dacey MF (1960) A note on the derivation of nearest neighbour distances. *J Regul Sci* 2(81):88. <https://doi.org/10.1111/j.1467-9787.1960.tb00842.x>
- DeMaria M, Kaplan J (1994) A statistical hurricane prediction scheme (SHIPS) for the Atlantic basin. *Weather Forecast* 9:209–220
- DeMaria M, Mainelli M, Shay LK, Knaff JA, Kaplan J (2005) Further improvements to the statistical hurricane intensity prediction scheme (SHIPS). *Weather Forecast* 20:531–543
- Dube SK, Rao AD, Sinha PC, Nahuleyan N (1997) Storm surge in Bay of Bengal and Arabian Sea: the problem and its prediction. *Mausam* 48:288–304
- Emanuel K (1988) The maximum intensity of hurricanes. *J Atmos Sci* 45:1143–1155
- Fofonff P, Millard RC Jr (1983) Algorithms for computation of fundamental properties of seawater, 1983. Unesco technical paper in marine science, vol 44, pp 53
- George JE, Gray MW (1976) Tropical cyclone motion and surrounding parameter relationship. *J Appl Meteorol* 15:1252–1264
- Gilson J, Roemmich D, Cornuelle B, Fu LL (1998) Relationship of TOPEX/Poseidon altimetric height to steric height and circulation of the North Pacific. *J Geophys Res* 103:947–965
- Goni GJ (2008) Tropical cyclone heat potential state of the climate in 2007. *Bull Am Meteorol Soc* 89:S43–S45
- Goni G, Kamholz S, Garzoli S, Olson D (1996) Dynamics of the Brazil-Malvinas confluence based on inverted echo sounders and altimetry. *J Geophys Res* 101:16273–16289
- Goni GJ, Garzoli SL, Roubicek AJ, Olson DB, Brown OB (1997) Agulhas ring dynamics from TOPEX/POSEIDON satellite altimeter data. *J Marine Res* 55:861–883
- Goni GJ, DeMaria M, Knaff JA, Sampson C, Ginis I, Bringas F, Mavume A, Lauer C, Lin I-I, Ali MM, Sandery P, Ramsos-buarque S, Kand K, Mehra A, Chassignet E, Halliwell G (2009) Applications of satellite derived ocean measurements to tropical cyclone intensity forecasting. *Oceanography* 22:176–183

- Gray M (1979) Hurricanes: their formation, structure and likely role in the tropical circulation. In: Shaw DB (ed) *Meteorology over the tropical oceans*. James Glaisher House, Bracknell, pp 155–218
- Griffies SM, Gnanadesikan A, Pacanowski RC, Larichev VD, Dukowicz JK, Smith RD (1998) Isonutral diffusion in a z-coordinate ocean model. *J Phys Oceanogr* 28:805830. [https://doi.org/10.1175/15200485\(1998\)028%3c0805:IDIAZC%3e2.0.CO;2](https://doi.org/10.1175/15200485(1998)028%3c0805:IDIAZC%3e2.0.CO;2)
- Harwood P, Scarratt R (2013) Tropical cyclone heat potential (TCHP) data handbook. 2.0:20
- Jangir B, Swain D, Udaya Bhaskar TVS (2016) Relation between tropical cyclone heat potential and cyclone intensity in the North Indian Ocean. In: *Proceedings on SPIE 9882, remote sensing and modelling of the atmosphere, oceans and interactions VI*, 988228-1-7; <https://doi.org/10.1117/12.2228033.ra>
- Kashyap T, Prasada Rao TDV, Agarwal S, Arulraj M, Ali MM (2012) Estimation of tropical cyclone heat potential on operational basis. NRSC technical report, NRSC-ECSA-AOSG-Sept-TR-442:7
- Knaff JA, Sampson CR, DeMaria M (2005) An operational statistical typhoon intensity prediction scheme for the western North Pacific. *Weather Forecast* 20:688–699
- Kumar B, Chakraborty A (2011) Movement of seasonal eddies and its relation with cyclonic heat potential and cyclogenesis points in the Bay of Bengal. *Nat Hazards* 59:1671–1689
- Leipper D, Volgenau D (1972) Hurricane heat potential of the Gulf of Mexico. *J Phys Oceanogr* 2:218–224
- Mainelli M, DeMaria M, Shay LK, Goni G (2008) Application of oceanic heat content estimation to operation forecasting of recent Atlantic category 5 hurricanes. *Weather Forecast* 23:3–16
- Mayer DA, Molinari LR, Baringer OM, Goni GJ (2001) Transition regions and their role in the relationship between sea surface height and subsurface temperature structure in the Atlantic Ocean. *Geophys Res Lett* 28:3943–3946
- Millero FJ, Poisson A (1981) International one-atmosphere equation of state of seawater. *Deep-Sea Res Part I* 28:625–629
- Millero FJ, Chen C-T, Bradshaw A, Schleicher K (1980) A new high pressure equation of state for Seawater. *Deep-Sea Res Part I* 27:255–264
- Nagamani PV, Ali MM, Goni GJ, Pedro ND, Pezzullo PC, Uday Bhaskar TVS, Gopalkrishna VV, Kurian N (2012) Validation of satellite-derived tropical cyclone heat potential with in situ observations in the North Indian Ocean. *Remote Sens Lett* 3:615–620
- Pun IF, Wu CR, Ko DS, Liu WT (2007) Validation and application of altimetry—derived upper ocean thermal structure in the Western North Pacific Ocean for typhoon—intensity forecast. *IEEE Trans Geosci Remote Sens* 45:1616–1630
- Ravichandran M, Behringer D, Sivareddy S, Girishkumar MS, Chacko N, Harikumar R (2013) Evaluation of the global ocean data assimilation system at INCOIS: the tropical Indian Ocean. *Ocean Model* 69:123–135
- Sadhuram Y, Ramana Murthy TV, Somayaajulu YK (2006) Estimation of tropical cyclones heat potential in the Bay of Bengal and its role in the genesis and intensification of storm. *Indian J Marine Sci* 352:132–138
- Sengupta D, Raj GNB, Senoi SSC (2006) Surface Freshwater from Bay of Bengal runoff and Indonesian throughflow in the tropical Indian Ocean. *Geophys Res Lett* 33:L22609. <https://doi.org/10.1029/2006GL027573>
- Sharma N, Ali MM (2014) Importance of ocean heat content for cyclone studies. *Oceanogr* 2:124. <https://doi.org/10.4172/2165-7866.1000124>
- Sharma N, Ali MM, Knaff JA, Chand P (2013) A soft-computing cyclone intensity prediction scheme for the Western North Pacific Ocean. *Atmos Sci Lett* 14:187–192
- Singh OP (2007) Long-term trends in the frequency of severe cyclones of Bay of Bengal: observations and simulations. *Mausam* 58:59–66
- Singh OP, Khan TMA, Rahman S (2000) Changes in the frequency of tropical cyclones over the North Indian Ocean. *Meteorol Atmos Phys* 75:11–20
- Singh OP, Khan TMA, Rahman MS (2001) Has the frequency of intense tropical cyclones increased in the North Indian Ocean? *Curr Sci* 80:575–580
- Song Q, Gorden AL, Visbeck M (2003) Spreading of the Indonesian throughflow in the Indian Ocean. *J Phys Oceanogr* 34:772–792
- Srivastav AK, Ray SKC, De US (2000) Trends in the frequency of cyclonic disturbances and their intensification over Indian seas. *Mausam* 51:113–118
- Sumesh KG, Ramesh KMR (2013) Tropical cyclones over North Indian Ocean during El-Nino Modoki years. *Nat Hazards* 68:1057–1074. <https://doi.org/10.1007/s11069-013-0679-x>
- Swain D, Krishnan VCN (2013) Prediction of depth of 26°C isotherm and tropical cyclone heat potential using a one-dimensional ocean model, Ver 1.0, National Remote Sensing Centre Technical Report. NRSC-ECSA-OSG-May2013-TR-529:28

- Valsala VK, Ikeda M (2005) Pathways and Effects of the Indonesian throughflow water in the Indian Ocean using particle trajectory and tracers in an OGCM. *J Clim* 20:2994–3017
- Venkatesan R, Shamji VR, Latha G, Mathew M (2013) In situ ocean subsurface time-series measurements from OMNI buoy network in the Bay of Bengal. *Curr Sci* 104(9):1166–1177
- Vissa NK, Satyanarayana ANV, Bhaskaran PK (2013) Response of oceanic cyclogenesis metrics for NAR-GIS cyclone: a case study. *Atmos Sci Lett* 14:7–13
- Wada A, Usai N (2007) Importance of tropical cyclone heat potential for tropical cyclone intensity and intensification in the western North Pacific. *J Oceanogr* 63:427–447
- Wada A, Usui N, Sato K (2012) Relationship of maximum tropical cyclone intensity to sea surface temperature and tropical cyclone heat potential in the North Pacific Ocean. *J Geophys Res*. <https://doi.org/10.1029/2012jd017583>
- Willis JK, Roemmich D, Cornuelle B (2004) Inter annual variability in upper-ocean heat content, temperature and thermocline expansion on global scales. *J Geophys Res*. <https://doi.org/10.1029/2003jc002260>
- Wong A, Keeley R, Carval T (2009) The Argo Data Management Team, Argo Data Management, version 2.5
- Zambresky L (1989) A verification study of the global WAM model, December 1987–November 1988, technical report no. 63. Reading, England: European Centre for Medium-Range Weather Forecasts, 90 <https://www.ecmwf.int/node/13201>

Publisher's Note Springer Nature remains neutral with regard to jurisdictional claims in published maps and institutional affiliations.

Affiliations

Babita Jangir¹  · D. Swain¹ · Samar Kumar Ghose¹ · Rishav Goyal¹ · T. V. S. Udaya Bhaskar²

¹ School of Earth, Ocean & Climate Sciences, Indian Institute of Technology Bhubaneswar, Argul Campus, Jatni, Odisha 752050, India

² Indian National Centre for Ocean Information Services (MoES), Pragathi Nagar, Hyderabad, Telangana 500090, India